High Resolution SAR Image Description by Combining the PCA and the Azimuth Sub-band Decompositions

Houda Chaabouni-Chouayakh[1] and Mihai Datcu[1,2]

[1] *German Aerospace Center (DLR), Oberpfaffenhofen D-82234 Wessling - Germany.*

[2] *Paris Institute of Technology, GET/Télécom Paris, 46 rue Barrault 75013 Paris - France*

Abstract With the increase of the Synthetic Aperture Radar (SAR) sensor resolution, a more detailed analysis and a finer description of SAR images are needed. However, in the case of urban areas, the high diversity of man-made structures combined with the complexity of the scattering processes make the analysis and information extraction from high resolution SAR images non-trivial. Moreover, the need for automatic processing and interpretation of large-size SAR data volumes has become more and more pressing. Therefore, new innovative tools are required for a better assessment and a finer description.

This paper proposes an automatic SAR image interpretation approach based on the marriage of two techniques: the Principal Components Analysis (PCA) and the azimuth sub-band decomposition. Indeed, both methods were proved to be of great interest in the analysis and modeling of the SAR image contents. Thus, a combination should be more informative and better descriptive. In this article, both a description of two combination ways that we propose to use, and a presentation of our preliminary performance results will be provided.

Keywords: High resolution SAR, information extraction, PCA, Azimuth sub-band decomposition.

1. Introduction

Satellite imagery has found vast applications in a wide spectrum of areas including urbanization (e.g. tracking the development of urban areas), cartography (e.g. detection of rivers, road networks), surveillance (e.g. detection and if possible recognition of military targets), etc. This heavy demand on satellite imagery applications leads to the development of imaging systems that are alternative to optical imagery. In particular, Synthetic Aperture Radar (SAR) imagery, in the last two decades, has become increasingly popular as some of its properties are favorable to optical imagery. SAR is a coherent imaging mode in the microwave domain ([1–3]) that can operate regardless of weather conditions, and whose resolution is independent of sensor height.

When dealing with urban areas, the electromagnetic scattering is characterized by a variety of single or multiple scattering mechanisms with a wide range of scattering amplitudes. Moreover, SAR images over urban areas are strongly affected by geometric distortion effects (as layover, shadowing) due to the combination of the SAR side-looking acquisition and stepwise height variations within the scene. This makes the interpretation and information extraction over such areas from SAR images more complex to perform.

With the increase of the SAR sensor resolution, high resolution SAR images could include a large variety of real man-made structures (buildings, roads, ground vehicles, etc) showing different backscattering behaviors, as described in [4]. A full understanding of the varying behaviors of all types of backscatterers becomes thus, not easily reachable. However, since the easiest geometrical structures characterizing urban areas are points and lines, we will focus in this paper on the automatic detection of strong targets/scatterers related in general to the presence of man-made structures.

To better characterize the backscattering behaviors of the different strong scatterers, sub-aperture techniques were found to be a powerful tool since it exploits at most the spectrum, which is very rich in the case of high resolution SAR images. In fact, application of such techniques involves the trade-off between azimuth resolution and temporal (view angle) dependencies. In [5–7], it was demonstrated that the azimuth sub-band decomposition often allows more detailed analysis of objects with directionally dependent backscatterers. This extra-information was proved to be quite useful to get a better characterization of the strong scatterers and to enhance some areas of interest. In [8], the spectral analysis of sub-bands was used to generate detected target maps, benefiting

of a contrast critically improved between a target and its environment. The same technique was also used in [9] for polarimetric and interferometric characterization and identification in urban areas of the so-called coherent scatterers (scatterers characterized by a deterministic point-like scattering behavior).

In the SAR Automatic Target Recognition (ATR), it is important to be able to reliably detect or classify a target in a manner which provides the largest possible robustness to target and clutter variability, with the highest possible discrimination capability. The SAR ATR methods were firstly developed mainly for surveillance applications (detection/characterization and if possible identification of very specific military targets of oppositional forces). But, high resolution SAR images, especially over urban areas, include currently a much larger spectrum of targets with respect to those used for military applications. Thus, the already developed surveillance ATR systems could no more be optimal for SAR ATR and new more suitable features should be used for a better understanding of urban areas. The high diversity propriety of urban areas, in comparison to military targets could be easily seen in Fig. 1.

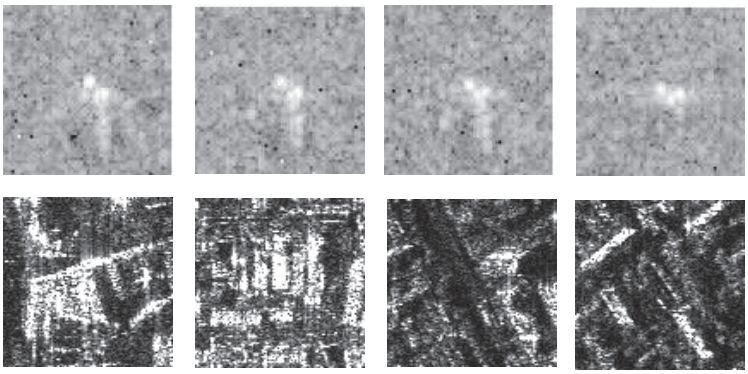

Fig. 1. First line: Some examples of the military MSTAR database (http://cis.jhu.edu/data.sets/MSTAR/). Second line: some examples of high resolution SAR images over the city of Dresden in Germany, acquired with the Experimental SAR system (E-SAR) of the German Aerospace Center (DLR).

Many approaches to performing ATR for data characterization have been proposed in the literature. Among ATR methods, the Principal Components Analysis (PCA) was proved to be quite promising. It is the most popular statistical method for feature extraction, based on the assumption that the most reliable information is stored in the directions to the maximum data variances. Since the maximal variances equal

the largest eigenvalues, the orthogonal basis generated by the PCA, is actually the subset of the eigenspace of the sample covariance matrix (eigenvectors corresponding to the largest eigenvalues).

PCA techniques were widely used to extract features from different kinds of images. For example, [11] proposes an unsupervised technique for visual target modeling, which is based on density estimation in high-dimensional spaces using PCA. Such an approach was proved to be well-suited for the detection of facial features. It exploits the redundancy to reduce the dimensionality of the training imagery, in order to form a computationally simple estimator for the complete likelihood function of the object. The estimator in this case, has the advantage that it is based on a subspace decomposition and can be evaluated using only the most principal component vectors. Like human faces, SAR images over urban areas provide a high diversity of features. Thus, a PCA based method should be also adapted to the recognition of the different structures existing in the urban SAR scenes. In [12], it was demonstrated that the eigenspace relative to the covariance matrix of the training images, provides a well-suited descriptive model of some specific SAR scenes. A PCA is performed on the training set in order to identify the eigen-images that provide the best discrimination between the different classes (called also the eigenspace). This approach was applied to radar target identification in a three-class database formed by tanks, Armored Personnel Carriers (APCs) and self-propelled guns. Such special targets are unfortunately not usual in high resolution SAR images over urban areas. In general, in urban areas, the mostly found classes consist rather in large/small buildings, vegetation, roads, parking, etc. Processing these classes is much more complex than tanks, APCs and guns, where the distribution variety of the targets is not too large.

In this paper, detection/characterization algorithms are developed for targets in high resolution SAR images by combining the promising properties of the azimuth sub-band decomposition with the ones of the PCA. Indeed, both methods were proved to be of great interest for different kinds of signals. Therefore, a combination should generate both relevant and reliable signatures/features that better model the SAR complicated behaviors of the targets that may exist in the scene.

A brief overview of the paper follows. Section 2 provides a description of the azimuth sub-band decomposition algorithm and its application for high resolution SAR image analysis. Section 3 is dedicated to the PCA formalism. Then, in section 4, two ways of combination between the PCA formalism and the azimuth sun-band decomposition, are exposed. Finally, section 5 summarizes the main results of our study.

2. Azimuth sub-band decomposition of high resolution SAR images

Several techniques of frequency analysis could be applied to a signal. For high resolution SAR images, the azimuth sub-band decomposition seems to be a promising tool to get a finer analysis of the different scatterers behaviors ([5–7]). The azimuth direction is along the flight axis and each position corresponds to some frequency variations due to the Doppler effect. Each point in the scene, is illuminated many times by the radar beam. A selection of an azimuth sub-aperture corresponds thus, to a selection of a range of viewing angles or sensor positions. It is thus worth to process the azimuth spectrum of high resolution SAR images for a more detailed understanding of the scene.

Due to both the particular fine backscattering phenomena in urban areas and the directivity property of the illuminated objects (depending on their orientations, the material of their surroundings surfaces, etc), the signal of a sub-band can be quite different from both, the full spectrum signal (original image) and the other generated sub-bands. For instance, rough surfaces are quasi-Lambertian and isotrope when the roughness is high according to the wavelength. Therefore, the same backscattering intensity should be observed in each sub-band. However, for some man-made objects in urban areas, such as a smooth wall or dihedre, the backscattered signal is highly dependant on the relative direction of the incidence wave and the object. In this case, the target could be faded or even disappear in some sub-bands.

The azimuth spectrum division could be done in n parts (sub-bands). In our work, for sake of simplicity, we chose to undergo a division of the spectrum into two, but the cases of $n > 2$ could also be studied. The 2 sub-band azimuth decomposition is made by the following steps:

- **Step 1:** Doppler centroid estimation and compensation of Doppler shift (in [13], three Doppler centroid estimators were proposed). For our experiment, we chose the frequency-domain estimation method which uses the symmetry axis of the spectrum propriety to provide an estimate of the Doppler centroid;
- **Step 2:** Unweighting in azimuth in order to obtain a uniform spectral density in the useful spectrum. In our work, we used a Hamming function to make the unweighting since a focused SAR image is usually weighted with a Hamming window;
- **Step 3:** Spectrum division into 2 sub-bands;

- **Step 4:** Centering the obtained sub-images; and finally
- **Step 5:** Zero-padding and Hamming weighting of each sub-band in order to suppress the sidelobes. This step is essential in urban areas due to the presence of many strong point-like scatterers.

It is noted that, the azimuth resolution of the regenerated signals is degraded by a factor of 2 according to the original resolution. The different steps of the 2-azimuth sub band decomposition algorithm are described in Fig. 2.

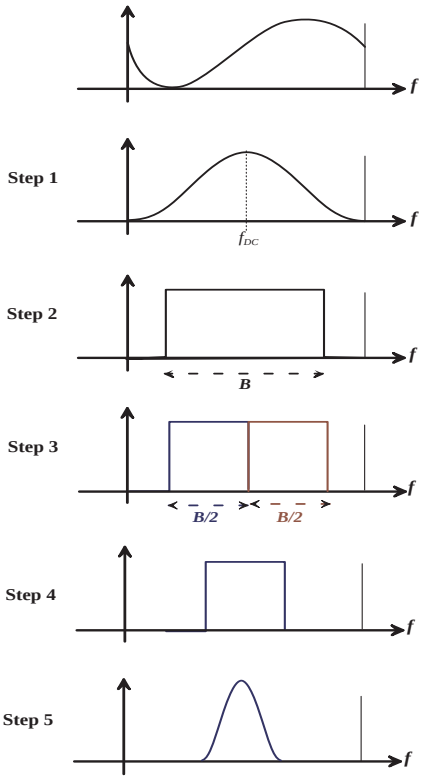

Fig. 2. Steps of the 2 sub-band azimuth decomposition.

Fig. 3 depicts the point-target analysis in the original SAR image and in the two obtained sub-bands. Both horizontal and vertical profiles at one exemplarily target are given in order to better study the behaviors of the targets regarding the orientation of the sensor.

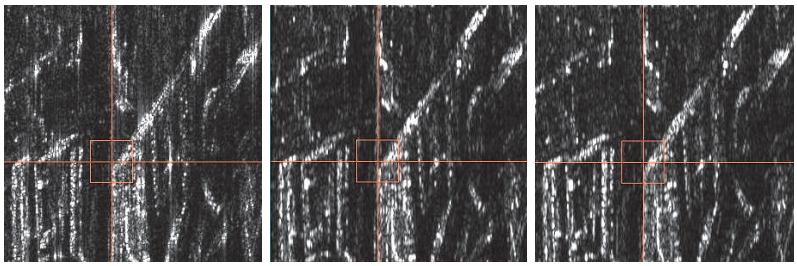

(a) Original image. (b) Sub-band left. (c) Sub-band right.

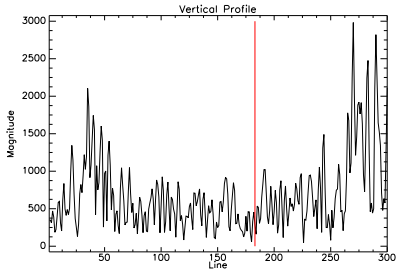

(d) Original image: Vertical profile.

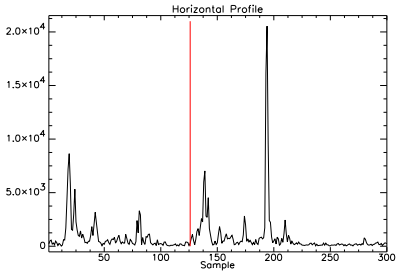

(e) Original image: Horizontal profile.

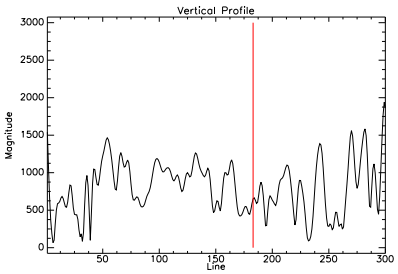

(f) Sub-band left: Vertical profile.

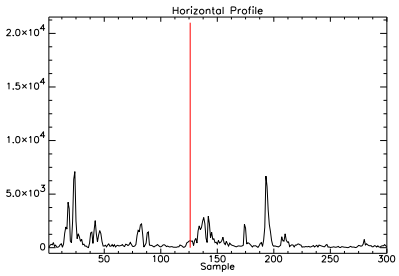

(g) Sub-band left: Horizontal profile.

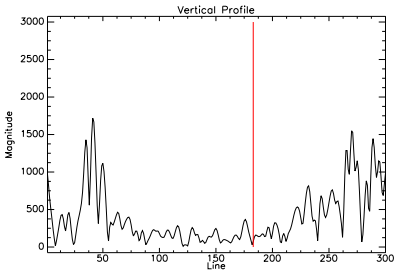

(h) Sub-band right: Vertical profile.

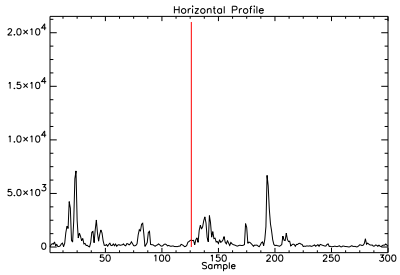

(i) Sub-band right: Horizontal profile.

Fig. 3. Point-target analysis of the original SAR image and its two sub-bands.

From Fig. 3, many interesting effects can be observed:

1 **Evidence of some details which were not in the original image:** Since the full-band image corresponds to a complex average of the zero-padded images, there are configurations where the structures do not appear at all in the full resolution image, although they are clearly seen in one of the sub-bands. For example, regarding the horizontal profiles, the contribution of the structure of the sample number 20 is stronger in the sub-band left than it was in the original image.

2 **Changing behaviors from one band to another:** The backscattering behavior could also change from the left to the right sub-band when the backscatter orientation is more adapted to a certain direction of the sensor than the other. For instance, we can notice the evidence of a vertical line in the sub-band left, which has a lower contribution in the original image and does not exist at all in the sub-band right. The vertical profiles drawn in Fig. 3(d,f,h) illustrate well this changing behavior.

3 **Stability of the corner reflectors:** The dihedral corner reflectors wall/ground of the buildings appear in all the sub-bands with high amplitudes. They are dihedrals on rough surfaces, their backscattering is lambertian and thus, it does not depend on the orientation or the position of the sensor. An example of such a behavior is illustrated by the three horizontal profiles of the sample number 194.

3. Principal Components Analysis (PCA)

Like all the feature extraction methods, PCA aims at extracting various image features for identifying or interpreting meaningful physical objects from images. It attempts to aggregate or combine the features in such a way to extract the common information contained in them that is the most useful for building the model. A model is called well-built if the signatures, that it provides from different classes, can be well-separated.

PCA is an orthogonal linear transformation that transforms the data to a new coordinate system such that the greatest variance by any projection of the data comes to lie on the first coordinate (called the first principal component), the second greatest variance on the second coordinate, and so on.

Given a set of N 2-D target images having n by n pixels, we can form a set of vectors $\{X_i\}$, where $X_i \in \mathcal{R}^{n^2}$ by lexicographic ordering of the pixel elements of each target image. Then, by considering the averaged images:

$$\bar{X}_i = X_i - \bar{X} \quad ; \quad i = 1, 2, ..., N \tag{1}$$

where $\bar{X}$ is assumed to be the average image defined as:

$$\bar{X} = \frac{1}{N} \sum_{i=1}^{N} X_i, \tag{2}$$

we can form the sample matrix $\bar{\bar{X}}$ as follows:

$$\bar{\bar{X}} = [\bar{X}_1, \bar{X}_2, ..., \bar{X}_N]. \tag{3}$$

The PCA transformation is given by:

$$Y = H^T \bar{\bar{X}}, \tag{4}$$

where:

- Y contains the transformed dimensional vector samples; and
- H is a $M \times M$ transform matrix. It is calculated from the eigenvectors of the covariance matrix $\Sigma = \frac{1}{N} \bar{\bar{X}} \bar{\bar{X}}^T$ of $\bar{\bar{X}}$. In fact, it is assumed, in this case, that most of the $\bar{\bar{X}}'$information content is stored in the directions of the maximum data variance, under the constraint of orthogonality. Since the M largest eigenvalues equal the maximal variances, the M corresponding eigenvectors are exactly the columns of the matrix H.

The PCA features are obtained by simple projections of all the images of the database (converted into vectors) in the eigenspace formed by the M most important eigenvectors.

In general, in the ATR systems, after the feature extraction step comes the classification step where a part of the database is used to train the classifier and the rest to test. To decide about the class of the test images, many existing classifiers could be used such as $k-$nearest neighbors ($k-nn$), Support Vector Machine (SVM), etc. However, since in this paper, our focus consists in image interpretation and since the classification step is carried out only to evaluate the quality of the extracted features, we have applied simply the $k-nn$ in our experiments. Thus, the projection vector (feature vector) of each test target is compared to all the training

feature vectors, and the class of this test vector is decided based on the k smallest distances from the class training vectors. An object is classified by a majority vote of its neighbors, with the object being assigned the class most common amongst its k nearest neighbors. If $k = 1$, then the object is simply assigned the class of its nearest neighbor.

Fig. 4 shows the flowchart of the PCA algorithm implementation.

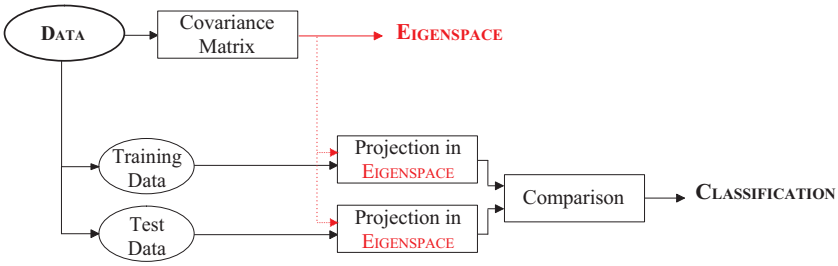

Fig. 4. Flowchart of the PCA algorithm.

4. Combination between the PCA and the azimuth sub-band decomposition

From section 2, we concluded that the azimuth sub-band decomposition of high resolution SAR images over urban areas, provides better information and finer description of man-made structures than when dealing only with the original images. Therefore, using combinations between the azimuth decomposition and the PCA transformation should lead to superior classification performance and better discrimination between the different classes. Two ways of combination are proposed in this paper:

- **Algorithm 1: A combination of the sub-bands followed by a PCA.** Like in our previous publication [14], instead of working directly on the full-spectrum images X_i $(i = 1, 2, ..., M)$, we propose to use X_i^{Az} $(i = 1, 2, ..., M)$ defined as follows:

$$X_i^{Az} = \begin{bmatrix} X_i^1 \\ X_i^2 \end{bmatrix} \quad ; \quad i = 1, 2, ..., M \tag{5}$$

  where X_i^k $(k = 1, 2)$ denote the two sub-bands (converted into vectors) obtained after a 2-azimuth sub-band decomposition of the original image X_i.

- **Algorithm 2: A combination of the PCA features of each sub-band.** In this case, the combination is rather performed after the PCA. If we assume that the principal components (features) extracted by applying a PCA on the first sub-band of the image X_i are stored in the vector PC_i^1 and the ones on the second sub-band in the vector PC_i^2, then the new feature vector of the image X_i would be:

$$PC_i = \begin{bmatrix} PC_i^1 \\ PC_i^2 \end{bmatrix}. \tag{6}$$

The flowcharts of the two combination algorithms are described in figures 5 and 6.

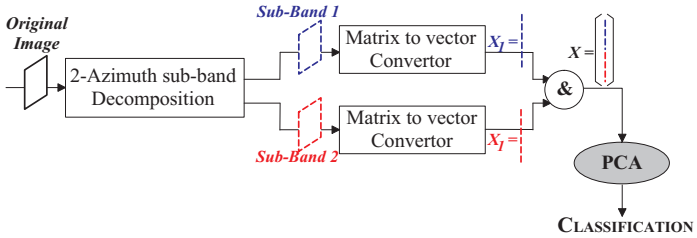

Fig. 5. Flowchart of **Algorithm 1**: A combination of the sub-bands followed by a PCA.

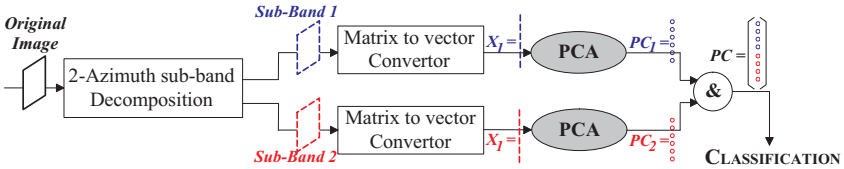

Fig. 6. Flowchart of **Algorithm 2**: A combination of the PCA features of each sub-band.

In order to get better classification results, we have performed a feature selection after the feature extraction step. In fact, this selection attempts to identify the best features among the available features, and thus leads to better performance results, by providing more suitable data modeling (good discrimination between the different classes), and speeding up the learning process (since we will work with a subset of the features).

5. Experimental Results

5.1 Description of the database

For our experiments, we used a five-class SAR database including:

- High Density urban areas (HD);
- Average Density urban areas (AD);
- Low Density urban areas (LD);
- Vegetation (V); and
- Water (W).

The size of the whole database is 250 images (50 images per class). One sample from each class is provided in Fig. 7.

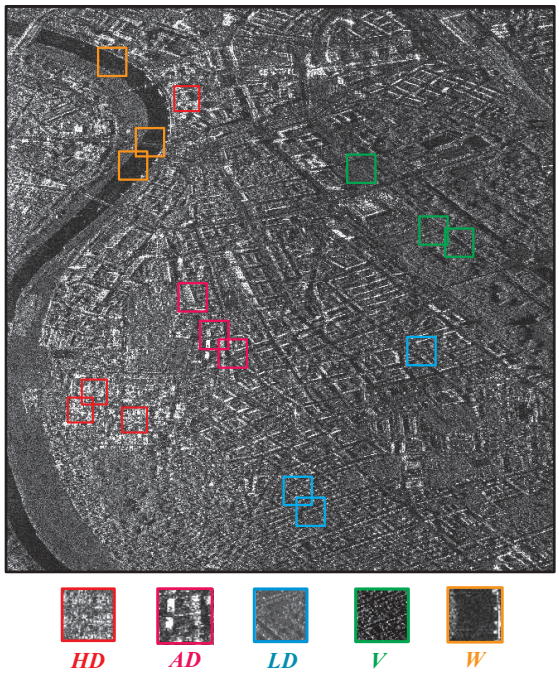

Fig. 7. High resolution SAR image over the city of Dresden in Germany and samples from each class.

They are intensity images, collected from the same Single Look Complex (SLC) SAR image, over the city of Dresden in Germany (August 2000), acquired with the airborne Experimental SAR system (E-SAR), of the German Aerospace Center (DLR). It is an X-band SAR image whose resolution is 1.5 m in the range direction, and equals 0.6 m in the azimuth direction.

5.2 Classification results

In order to stress the importance of the use of both the PCA formalism and the azimuth sub-band decomposition, we have carried out a classification performance comparison, between the following five experiments:

- PCA performed directly on the original images;
- PCA performed only on the sub-bands 1;
- PCA performed only on the sub-bands 2;
- **Algorithm 1**: a combination of the two sub-bands followed by a PCA; and finally
- **Algorithm 2**: a combination of the PCA features extracted from each sub-band.

It is worth to note that for the four first algorithms, we restrained the total number of features to 7 (projections of the test images in the eigenspace composed by the 7 eigenvectors corresponding to the 7 largest eigenvalues). In fact, over 7 components, the feature selection process gets very slow (more computational effort). However, in the case of the 5^{th} experiment, the selection of the most reliable features is performed on a 14 element-feature vector; composed by the 7 PCA features extracted from the sub-bands 1 combined with the 7 PCA features extracted from the sub-bands 2.

For each of our experiment, we chose to make 5 repetitions with randomly selected train and test datasets. For each repetition, 50% of the data is used for training the classifier and the rest for testing. This technique is called the cross-validation. It aims at estimating how well the model, we have just learned from some training data, is going to perform on future as-yet-unseen data. By applying such an approach, we avoid any possible dependency between the training dataset and the classification performance.

The recognition rates (averages and standard deviations of 5 repetitions), that could be obtained by each algorithm if a perfect selection of components is carried out, are shown in Fig. 8.

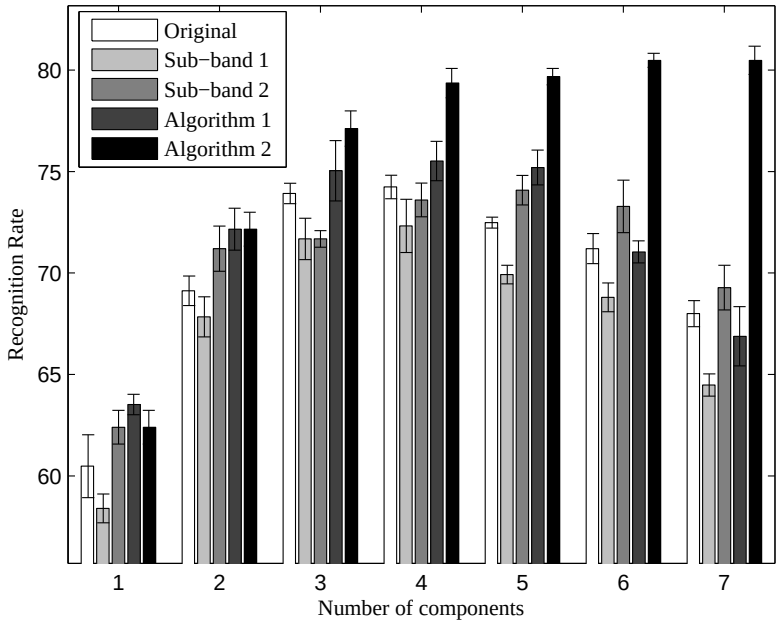

Fig. 8. Classification performances of PCA on the original images, PCA on the sub-bands 1, PCA on the sub-bands 2, **Algorithm 1** and **Algorithm 2**: Recognition rates as a function of the number of components, when considering feature selection.

The following observations could be made from the classification results summarized in Fig. 8:

- Unlike the case of the PCA applied only on the sub-bands 1, the one performed on the sub-bands 2 gives, in most of the cases (number of selected components in $[1, 2, 5, 6, 7]$) better classification results, than when working directly on the original images. This means that the information stored in the second sub-bands, generate some useful details which were not in the original images. These details seem to characterize more the contents of the different classes and

discriminate better between them. The evidence of such details in the sub-bands 2, is probably due to the fact that, the sensor direction in this case, is more adapted to the orientation of the backscatters that exist in the scene.

- It seems that the information given by the sub-bands 1, generates a kind of confusion between the different classes. In fact, among our five experiments, the worst recognition rates were obtained when the PCA formalism was performed only on the sub-bands 1. Moreover, for a high number of selected components (6 and 7), the combination between the information stored in the two sub-bands (**Algorithm 1**) did not improve the classification results. Indeed, a PCA performed only on the sub-bands 2 was discriminating better between the different classes of our database.
- The recognition rates are highly dependent on the number of selected components. In fact, by selecting the most relevant and the less redundant features, we not only provide a more suitable data modeling (better classification results for the five algorithms), but also we speed up the learning process (less computational effort in the classification/comparison step).
- Both combination algorithms are worthwhile. In fact, by carrying out a perfect selection of the components, we could reach more than 75% of good classification for **Algorithm 1**, and more than 80% for **Algorithm 2**.
- For **Algorithm 1**, the best performances were obtained when only 4 features were chosen. The corresponding confusion matrix is given by table 1.

Table 1. Classification confusion matrix showing the performance of the classifier described in **Algorithm 1**, when the best subset of 4 features was selected.

	HD	AD	LD	V	W
HD	84%	6.4%	1.6%		
AD	14.4%	63.2%	29.6%	4%	
LD	1.6%	26.4%	52.8%	16.8%	
V		4%	16%	76.8%	0.8%
W				2.4%	99.2%

- **Algorithm 2** outperforms advantageously all the other algorithms. More particularly, when the number of selected components is high,

the recognition rates are clearly better than all the other algorithms (could reach more than 80%). The confusion matrix showing the performance of **Algorithm 2**, when the number of selected components equals 6 and 7, are respectively summarized in tables 2 and 3.

Table 2. Classification confusion matrix showing the performance of the classifier described in**Algorithm 2**, when the best subset of 6 features was selected.

	HD	AD	LD	V	W
HD	82.4%	4%			
AD	16.8%	68.8%	13.6%		
LD	0.8%	21.6%	60.8%	7.2%	
V		5.6%	25.6%	90.4%	
W				2.4%	100%

Table 3. Classification confusion matrix showing the performance of the classifier described in **Algorithm 2**, when the best subset of 7 features was selected.

	HD	AD	LD	V	W
HD	84%	2.4%			
AD	15.2%	65.6%	16%		
LD	0.8%	26.4%	62.4%	7.2%	
V		5.6%	21.6%	90.4%	
W				2.4%	100%

- From the three confusion matrix stored in tables 1, 2 and 3, it is clear that:
  - The best-recognized class (water) is well-discriminated from the rest of the database (almost 100% of good classification in all the cases).
  - The worst-recognized classes are the average and low density urban areas. Indeed, the contents of these two classes are non-trivial to identify, due to their high diversity and variability. More specific features are needed in this case.
  - The urban areas are quite mistaken between each other (mainly the high with the average density, and the average with the low one). This confusion is probably due to the fact that these

three classes include almost the same sub-structures (buildings, vegetation or gardens, roads, cars, etc) with different occurrences.

– The class of vegetation is mainly confused with the one of low density urban areas. Indeed, this former class includes in general the sub-class vegetation (gardens around some small buildings) among their surrounding area, which results in a kind of confusion.

– In the case of the average and low density urban areas, as well as, the vegetation, the combination made according to **Algorithm 2**, is more suitable than the one described in **Algorithm 1**, more notably for vegetation where a gain of around 15% could be achieved. However, for the high density urban areas and water, the two combination algorithms perform nearly the same.

– If we measure the classification performance by the highest lowest recognition rate (the best worst case), the classifier of the **Algorithm 2**, when the best subset of 7 features (among the 14 PCA features) is chosen, would come over (62.4% for the low density urban areas class).

6. Conclusions

In this article, a preliminary classification of high resolution SAR images has been performed on a five-class database (high density urban areas, average density urban areas, low density urban areas, vegetation and water).

The proposed method aims at exploiting the rich information provided by the azimuth sub-band decomposition and to combine it with the promising properties of the PCA, in order to get both a superior classification performance and a better discrimination between the different classes. Following this approach, two algorithms were proposed. The first one consists in a combination of the two sub-bands followed by a PCA, while the second one is rather a combination in the feature space (PCA features of the two sub-bands). It was demonstrated that the combination of the PCA features of the two azimuth sub-bands is globally, more beneficial and gives the highest recognition rates, when a perfect selection of the components is carried out (more than 80% of good classification).

The advantage of the feature selection process was also highlighted in this paper. In fact, selecting only the most relevant and the less redundant features makes the modeling of the data more appropriate, and the learning process faster.

Acknowledgment

This work was performed in the frame of the competence center CNES/DLR/ENST on information extraction and image understanding for earth observation (`http://www.coc.enst.fr/`).

References

[1] G. Schreier. *SAR Geocoding: Data and Systems.* Wichmann Verlag, pp. 53-102, 1993.

[2] C. Elachi. *Introduction to the Physics and Techniques of Remote Sensing.* John Wiley & Sons, pp. 176-220,1987.

[3] C.V. Jakowatz, D.E. Wahl, P.H. Eichel, D.C. Ghiglia, P.A. Thompson. *Spotlight-mode Synthetic Aperture Radar: A Signal Processing Approach.* Kluwer Academic Publishers, pp. 1-31, 1996.

[4] A.W. Rihaczek and S.J. Hershkowitz. *Radar Resolution and Complex-Image Analysis.* Artech House, pp. 17-68, 1996.

[5] H. Chaabouni and M. Datcu. Relevant Scatterers Characterization in SAR Images. In *Bayesian Inference and Maximum Entropy Methods in Science and Engineering*, pp. 375-382, Paris, France, July 2006.

[6] C. Tison. *Interférométrie RSO à Haute Résolution en Milieu Urbain: Application au Calcul de MNS Urbain.* Ph-D thesis, Ecole Nationale Supérieure des Télécommunications, France, 2004.

[7] F. Tupin and C. Tison. Sub-aperture Decomposition for SAR Urban Area Analysis. In *EUSAR 2004*, Ulm, Germany, May 2004.

[8] J.C. Souyris, C. Henry and F. Adragna. On the Use of Complex SAR Image Spectral Analysis for Target Detection: Assessment of Polarimetry. *IEEE Transactions on Geoscience and Remote Sensing*, VOL. 41, NO. 12, pp. 2725-2734, December 2003.

[9] R.Z. Schneider, K.P. Papathanassiou, I. Hajnsek and A. Moreira. Polarimetric and Interferometric Characterization of Coherent Scatterers in Urban Areas. *IEEE Transactions on Geoscience and Remote Sensing*, VOL. 44, NO. 4, pp. 971-984, April 2006.

[10] H.S. Kim. *Adaptative Target Detection in Radar Imaging.* Ph-D thesis, University of Michigan, 2001.

[11] B. Moghaddam and A. Pentland. A Subspace Method for Maximum Likelihood Target Detection. *IEEE International Conference on Image Processing*, Washington DC, 1995.

[12] L.M. Novak and G.J. Owirka. Radar Target Identification Using an Eigen-Image Approach. *IEEE National Radar Conference*, Atlanta, GA, 1994.

[13] S.N. Madsen. Estimating the Doppler Centroid of SAR Data. *IEEE Transactions on Aerospace and Electronic Systems*, VOL. AES-25, NO. 2, pp. 134-140, March 1989.

[14] H. Chaabouni-Chouayakh and M. Datcu. Azimuth Sub-band and Eigenspace Decomposition for High Resolution SAR Image Analysis. In *the fourth IEEE International Multi-conference on Systems, Signals and Devices (SSD'07)*, Hammamet, Tunisia, March 2007.